The H2O–CO2 continuum around 3.1, 5.2 and 8.0 μm: New measurements and validation of a previously proposed χ factor

Wissam Fakhardji, Ha Tran, Olivier Pirali, Jean-Michel Hartmann

Highlights

The $H_2O - CO_2$ continuum around 3.1, 5.2 and 8.0 µm: New measurements and validation of a previously proposed χ factor

Wissam Fakhardji, Ha Tran, Olivier Pirali, Jean-Michel Hartmann

- $H_2O - CO_2$ continuum measurements at room temperature
- Confirmation of previous measurements for the 1400 – 1500 cm^{-1} spectral region
- New measurements in the 1800 – 2000 and 3100 – 3300 cm^{-1} regions
- Validation of a previous χ factor model

The $H_2O - CO_2$ continuum around 3.1, 5.2 and 8.0 µm: New measurements and validation of a previously proposed χ factor

Wissam Fakhardji[a,*], Ha Tran[a], Olivier Pirali[b,c], Jean-Michel Hartmann[a]

[a] *Laboratoire de Météorologie Dynamique/IPSL CNRS, Ecole polytechnique, Institut polytechnique de Paris, Sorbonne Université, École normale supérieure, PSL Research University, Palaiseau, F-91120, France*
[b] *AILES beamline, SOLEIL Synchrotron, L'Orme des Merisiers, Saint-Aubin, 91190, France*
[c] *Université Paris-Saclay, CNRS, Institut des Sciences Moléculaires d'Orsay, Orsay, 91405, France*

Abstract

The $H_2O - CO_2$ continuum has been measured, at room temperature, at discrete spectral points in the 1100 – 1500, 1800 – 2000, and 3100 – 3300 cm^{-1} intervals. Our results are in good agreement with previous experimental values in the low frequency wing of the ν_2 band of H_2O when the associated uncertainties are taken into account. Furthermore, they confirm the quality, in this region, of a χ factor previously adjusted on measurements in the 100 – 1500 cm^{-1} range, and prove its validity in the blue side of the ν_2 band as well as in the region around 3.1 µm, which have been experimentally studied for the first time in this work. Together with recent measurements in the 1.6 µm, 2.3 µm and far infrared regions, our results contribute to the progressive building-up of a data set for the modeling of the absorption by $CO_2 + H_2O$ mixtures throughout the infrared, which is needed for studies of CO_2-rich planetary atmospheres.

Keywords: $CO_2 - H_2O$ continuum, measurements, χ-factor model, CO_2-rich atmospheres

*Corresponding author: wissam.fakhardji@lmd.ipsl.fr

1. Introduction

The accurate knowledge and modeling of spectra of $H_2O + CO_2$ mixtures for various temperature and pressure conditions is required for planetary science. In particular, the effect of CO_2 on the water vapor greenhouse effect must be known to model the atmospheres of Venus and Early Mars and it will likely be soon needed for some exoplanets [see, e.g. (Lebonnois et al., 2015; Turbet et al., 2021; Turbet et al., 2020; Pluriel et al., 2019)].

The absorption by gas samples containing water vapor is generally split into several contributions, which, in the present case of $H_2O + CO_2$ mixtures, are those of the local lines of the H_2O and CO_2 monomers, and those of the so-called continua associated with intermolecular interactions within $H_2O - H_2O$, $CO_2 - CO_2$ and $H_2O - CO_2$ pairs. This separation, which was introduced many years ago [see, e.g. (Burch, 1982; Burch and Alt, 1984)] and kept since then (Mlawer et al., 2012), has a practical interest since the continua are proportional to the product of the densities of the molecules involved (provided that the local transitions contributions are computed up to a distant to the line centers significantly larger than the pressure broadened widths). Recall that the continua potentially include contributions of the far wings of the pressure-broadened absorption lines of the monomers, of collision-induced absorption, and of bound and quasi-bound bi-molecular complexes.

In a pioneer study carried three decades ago, a quasistatic theoretical approach was developed (Ma and Tipping, 1992; Pollack et al., 1993) for the prediction of the $H_2O - CO_2$ continuum due to the far wings of the CO_2-broadened lines of H_2O. In the absence of any experimental results, the associated calculated spectra and line-shape correction-factor $\chi_{H_2O-CO_2}$ provided the very first data throughout the infrared. Twenty five years later came the first measurements of the $H_2O - CO_2$ continuum, which investigated the 1100–1300 cm^{-1} region (Baranov, 2016). Then, Tran et al. (2019) produced new data from 100 to 1500 cm^{-1}, which confirmed the results of Baranov (2016) and extended the investigated spectral range. Note that this latter study also provided a line-shape factor $\chi_{H_2O-CO_2}$ for CO_2-broadened H_2O transitions, obtained by adjusting the measured values between 100 and 1500 cm^{-1}, with which the calculated continuum agrees well with the experiments. For the H_2O-broadened wings of CO_2 lines, the situation is somehow similar, with first results and data obtained only recently. These include measurements in the high frequency wing of the CO_2

ν_3 band (Baranov, 2016; Tran et al., 2018) from which a $\chi_{CO_2-H_2O}$ absorption factor was deduced (Tran et al., 2018), and direct predictions using molecular dynamics simulations (Hartmann et al., 2018a). Finally, recall that another process participating to the continua is collision-induced absorption (CIA) (Frommhold, 1993). In the particular case of $H_2O + CO_2$ mixtures such a contribution was pointed out recently by a cavity ring down spectroscopy study (Fleurbaey et al., 2022a). This investigation, which provided values of the continuum of $H_2O + CO_2$ mixtures at some points around 1.60, 2.3 and 3.5 µm, also evidenced the presence of a CIA peak around 6000 cm^{-1}. The latter was soon after attributed (Fleurbaey et al., 2022b) to the simultaneous transitions involving the ν_3-band dipole of CO_2 and the ν_1-band polarizability of H_2O.

In the present work, we continue the efforts made to build up a $H_2O + CO_2$ continuum throughout the infrared by measuring the absorption, at room temperature, on both sides of the ν_2 band as well as around 3.1 µm. The experimental procedure is presented in Section 2 and the data analysis is described in Section 3. Finally, the results are shown in Section 4 and compared to previous experiments and predictions based on the line-shape factor $\chi_{H_2O-CO_2}$ proposed in Tran et al. (2019).

2. Measurements

The spectra were measured using the facilities at the AILES beam line of the SOLEIL synchrotron, previously used for similar experiments (Tran et al., 2019; Fakhardji et al., 2022). A high resolution Fourier transform spectrometer (FTS, Bruker IFS 125 HR) was used, equipped with a globar source and a KBr beam splitter. The light exiting the FTS passed through a 2.5 m long multi-pass cell with diamond windows, set for an optical path of 101.3 m. The transmitted intensity was then measured with a liquid nitrogen-cooled HgCdTe detector. For each spectrum, whose usable part lies between about 700 and 4600 cm^{-1}, an average of 1000 scans was made with an unapodized resolution of 0.5 cm^{-1}. In the measurements of the absorption by $H_2O + CO_2$ mixtures, all carried at 295 K, the cell was first filled with purified water vapor at a pressure of $\sim$ 15 mb (measured using a 0-1000 mb Pfeiffer model CMR361 capacitive gauge which has a stated accuracy of 0.2%). Then CO_2 was introduced step by step, progressively increasing the total pressure from $\sim$ 500 mb to $\sim$ 1000 mb (measured using the same capacitive gauge) and a spectrum was recorded after each step (awaiting

about 10 to 15 min each time to allow the gas mixture to reach equilibrium). In addition to this "ascendant" procedure, we also recorded spectra using a "descendant" procedure, i.e. starting from the highest pressure of $\sim$ 1000 mb and progressively reducing it down to $\sim$ 500 mb. Note that these two ways of collecting data are not equivalent since the mole fractions of H_2O ($\sim$ 1.5%) and CO_2 ($\sim$ 98.5 %) are kept constant in the descendant procedure while they vary in the ascendant one (the proportion of water vapor then decreasing from $\sim$ 3% down to $\sim$ 1.5%). In order to obtain the 100% transmittance levels, reference spectra were also recorded with the cell filled with pure argon at $\sim$ 1 bar, before and after each of the series with $H_2O + CO_2$ mixtures described above.

3. Data analysis

In a first step, the transmission associated with each $H_2O + CO_2$ sample was obtained by dividing the corresponding recording by the reference spectrum (recorded with argon). Then, various contributions to the absorption needed to be removed in order to obtain the targeted continuum due to the CO_2-broadened far wings of the H_2O lines. Indeed, for a CO_2+H_2O mixture at temperature T with densities d_{CO_2} and d_{H_2O}, the total absorption coefficient α_{tot} at wavenumber σ can be written as:

$$\begin{aligned}\alpha_{tot}(\sigma, d_{CO_2}, d_{H_2O}, T) = \alpha_{loc}^{CO_2}(\sigma, d_{CO_2}, d_{H_2O}, T) + \alpha_{loc}^{H_2O}(\sigma, d_{CO_2}, d_{H_2O}, T) \\ + \alpha_{CA}^{CO_2-CO_2}(\sigma, d_{CO_2}, T) + \alpha_{CA}^{H_2O-H_2O}(\sigma, d_{H_2O}, T) \\ + \alpha_{CA}^{H_2O-CO_2}(\sigma, d_{CO_2}, d_{H_2O}, T)\end{aligned} \quad (1)$$

where $\alpha_{loc}^{CO_2}$ and $\alpha_{loc}^{H_2O}$ are the contributions of local lines of the two molecules, computed including all transitions within a given interval (see below) around the current wavenumber. The coefficient $\alpha_{CA}^{CO_2-CO_2}$ and $\alpha_{CA}^{H_2O-H_2O}$ denote the continuum absorptions by pure CO_2 and H_2O respectively. Finally $\alpha_{CA}^{H_2O-CO_2}$ is the continuum absorption due to interacting $H_2O + CO_2$ pairs. In order to deduce $\alpha_{CA}^{H_2O-CO_2}$ we have computed all the other contributions as described below.

1 – Computation of the local lines absorption ($\alpha_{loc}^{CO_2}$, $\alpha_{loc}^{H_2O}$) – The calculation of the associated absorption coefficients was carried using Voigt profiles [truncated $\pm$ 5 cm^{-1} for CO_2, for consistency with Perrin and

Hartmann (1989) and ± 25 cm^{-1} for H_2O, for consistency with Mlawer et al. (2012) and Clough et al. (1989), away from their centers] with line positions and intensities taken from the HITRAN database (Gordon et al., 2022). Since the latter provides only self- and air-broadening coefficients, the needed values of the broadenings of H_2O lines by CO_2 were taken from Brown et al. (2007), while we used the data of Sung et al. (2009) for the H_2O broadenings of CO_2 transitions, as done in Tran et al. (2019). The pressure shifts of the CO_2 lines induced by collisions with H_2O and those of H_2O lines by CO_2 being not available, they are considered to be the same as the ones with air. The impact of this approximation is expected to be negligible given the small value of the line shift in comparison to the spectral resolution of the recorded spectra. The partial pressure of H_2O for each recording was also determined by fitting some absorption lines. The obtained results are consistent (with a difference around only $\sim 2\%$) with the values deduced from the H_2O mole fraction and the total pressure of the mixture (both a priori known through the pressure readings during the making of the mixture and the successive recordings).

2 – Computation of the pure CO_2 continuum ($\alpha_{CA}^{CO_2-CO_2}$) – $\alpha_{CA}^{CO_2-CO_2}$ was computed taking into account two contributions. The first, due to the wings of CO_2 lines broadened by collisions with CO_2, was computed using the $\chi_{CO_2-CO_2}$ factor from Perrin and Hartmann (1989). Note that this model was preferred to a line-mixing model because it leads to much better agreement with the measurements in the line-wings (Tran et al., 2011). The second, due to two collision-induced absorption bands around 1350 cm^{-1} (Baranov and Vigasin, 1999) was taken from Karman et al. (2019).

3 – Computation of the pure H_2O continuum – Finally, the contribution of the H_2O self-continuum was computed using the version v3.2 (available at http://rtweb.aer.com/continuum_frame.html) of the MT_CKD model (Mlawer et al., 2012).

Note that, since data are available for its computation, the contribution of the H_2O-broadened wings of CO_2 lines were computed using the $\chi_{CO_2-H_2O}$ from Tran et al. (2018), and removed from $\alpha_{CA}^{H_2O-CO_2}(\sigma, d_{CO_2}, d_{H_2O}, T)$. Note that it makes a practically negligible contribution in the investigated spectral regions.

Once all these contributions have been calculated, the associated spectral transmission $\tau_{Calc}(\sigma)$ is predicted and convolved by the FTS instrument function $F_{inst}(\sigma)$. The targetted continuum due to the far wings of the CO_2-broadened H_2O monomer lines was then obtained from the measured

transmission $\tau_{Meas}(\sigma)$ by using:

$$\alpha_{CA}^{H_2O-CO_2}(\sigma) = -ln\left[\tau_{Meas}(\sigma)/(\tau_{Calc}(\sigma) * F_{inst}(\sigma))\right]/L \quad (2)$$

where L is the optical path in cm and $*$ denotes a convolution. Note that for consistency with the usual definition of the H_2O continua (Mlawer et al. 2012; Clough et al., 1989), the values of $\alpha_{CA}^{H_2O-CO_2}(\sigma, d_{CO_2}, d_{H_2O}, T)$ provided by this procedure are corrected by adding the "pedestal" (since it was not substracted from $\alpha_{loc}^{H_2O}$) defined by:

$$P(\sigma, d_{CO_2}, d_{H_2O}, T) = \frac{d_{CO_2} d_{H_2O}}{\pi} \sum_{l \text{ if } |\sigma-\sigma_l|<25} \frac{S_l(T)\gamma_l(T)}{(25)^2} \quad (3)$$

where the sum extends over all H_2O lines centered within $\pm$ 25 cm^{-1} around the current wavenumber. $S_l(T)$ is the the integrated intensity of line l in cm^{-2}/amagat, and $\gamma_l(T)$ (in cm^{-1}.amagat^{-1}) is the CO_2-broadening coefficient of the line. Note that the amagat density unit is used here as in previous studies, 1 amagat corresponding to 2.687×10^{19} molec/cm^3.
Using the above described procedure, the $\alpha_{CA}^{H_2O-CO_2}$ continuum can potentially be retrieved for each wavenumber where the absorption by H_2O is measurable under our experimental conditions. However, the values obtained are very uncertain when the computed absorption that has been removed represents a very large part of the total absorption. Hence, as done in Tran et al. (2019), we selected only the spectral points located in troughs between lines and sufficiently distant from the latter. In order to determine the density-normalized $CA^{H_2O-CO_2}(\sigma, T)$ continuum from the values of $\alpha_{CA}^{H_2O-CO_2}(\sigma, d_{CO_2}, d_{H_2O}, T)$, we used the fact that, for binary collisions (an assumption valid at the pressures of our measurements), they are related through:

$$\alpha_{CA}^{H_2O-CO_2}(\sigma, d_{CO_2}, d_{H_2O}, T) = d_{CO_2} d_{H_2O} CA^{H_2O-CO_2}(\sigma, T) \quad (4)$$

We thus performed a linear fit of $\alpha_{CA}^{H_2O-CO_2}$ versus the product of the densities $d_{CO_2} d_{H_2O}$ for each retained spectral point. Some examples of this exercise are displayed in Fig. 1, which shows that our measured values do quite well follow the proportionality law of Eq. (4). Note that, in order to obtain these results, the level of the reference spectrum (corresponding to the 100% transmittance recorded with the cell filled with argon) was also adjusted by multiplying it by a linear function of wavenumber assumed independent of the pressure.

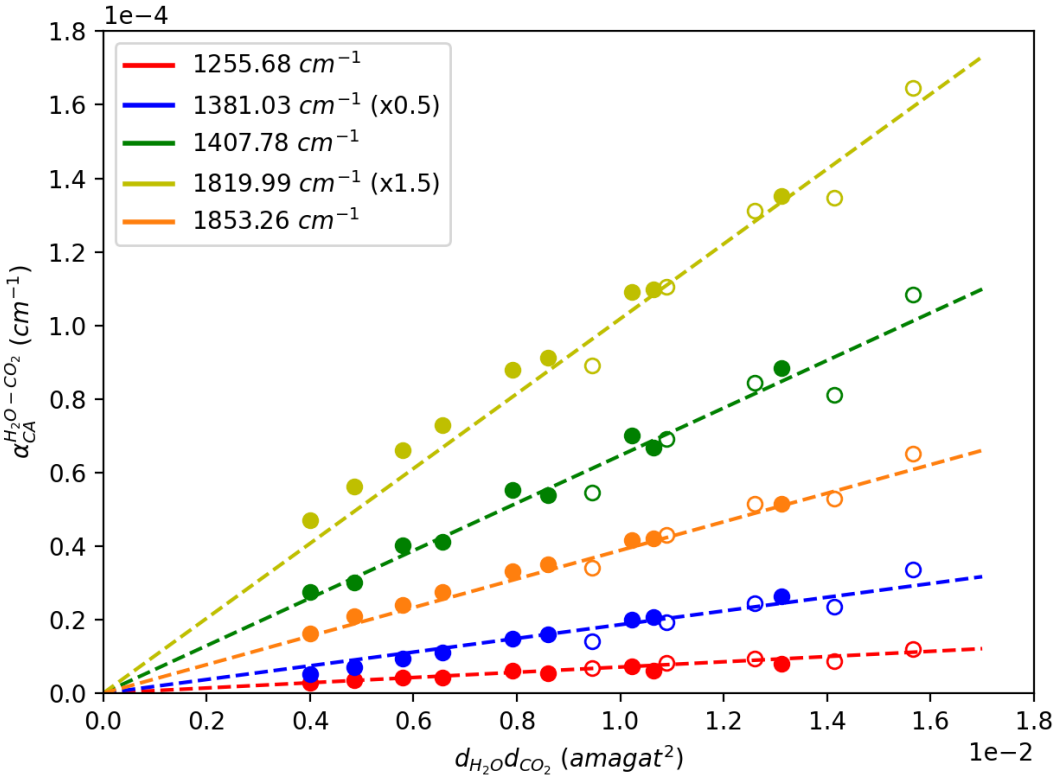

Figure 1: Examples of linear fits (dashed lines) of the measurements (represented with filled and empty dots respectively for increasing and decreasing pressure ramps) for fixed values of the wavenumber. The value of the $H_2O - CO_2$ continuum $CA^{H_2O-CO_2}(\sigma)$ is directly given by the slope of the line.

4. Results and discussion

Figure 2 displays a comparison of our experimental values (provided in the supplementary material) for the $H_2O - CO_2$ continuum with the other measurements available in the considered spectral region (Baranov, 2016; Tran et al., 2019). The uncertainties on our determinations, shown by the error bars in Fig. 2, were obtained taking into account three major sources of error. The first one comes from the dispersion of the measurements and it was obtained from the 1σ statistical error in the linear fits exemplified in Fig. 1. In addition, the calculations of the other contributions to the absorption (presented in Sec. 3) that have been removed propagate errors

due to uncertainties on the spectroscopic parameters used (in particular for the contribution of the H_2O local lines). This additional source of errors was computed using the uncertainties on the H_2O line intensities and air-broadening coefficients provided, for each line, by the HITRAN database (Gordon et al., 2022) [we thus assumed the same values for the CO_2-broadening coefficients of Brown et al. (2007)]. Even though they are not expected to play a major role, the uncertainties on the intensities and self-broadening coefficient for CO_2 are also taken in account. For both H_2O and CO_2 lines, we disregarded the uncertainties on their positions since the associated uncertainties are negligible. The third source of error is the uncertainty on the self H_2O continuum that we estimated by comparing the MT_CKD model with the measurements made by Ptashnik et al., (2019). The difference observed was on average about ~ 10 % and we then supposed this level for the uncertainties and added them to the error bars. Note that the first and the two other sources of error mentioned above behave differently according to the spectral region of interest. Indeed, the dispersion of the measurements becomes less important as the absorption increases, and the associated statistical error decreases. In contrast, the uncertainties on the spectral parameters and those on the self H_2O continuum naturally play a larger role near the center of the ν_2 band, while their impact is less pronounced in the far wings regions. Hence the first source of error dominates in the weak absorption regions, while the uncertainty associated with the calculation of the removed absorption is predominant near the band center. Finally, in our results we have selected only the values of the continuum which are larger than their associated uncertainty.

The first thing to be noticed is that, between 1100 and 1200 cm^{-1}, our continuum values are on average larger than the previous measurements (Baranov, 2016; Tran et al., 2019) (although all are compatible when uncertainties are taken into account) while at higher frequencies in the red wing of the ν_2 band the agreement is better. The center of the ν_2 absorption band being saturated it is not possible to extract information on the continuum but, in the 1800 – 2000 cm^{-1} range we were able to determine it, providing the first determination of the $H_2O - CO_2$ continuum, which is also the case for the 3100–3300 cm^{-1} interval.

As is well known, the self and foreign H_2O continua include four contributions, all proportional to the product of densities of the species involved: (i) What is left of the wings of the pressure-broadened monomer lines after the removal of the contribution of the transitions within $\pm$ 25

cm^{-1}. (ii) The absorption due to the interaction-induced dipole within free colliding pairs (see e.g. Fleurbaey et al., 2022a,b). The participation of (iii) bound and (iv) meta-stable or quasi-bound dimers. In the case of the water vapor continua the related importance of these four contributions has been a controversial and still open issue for decades (see e.g. Hartmann et al., 2018b and references therein), whose discussion is largely beyond the scope of the present study. However, an empirical approach was proposed by Tran et al. (2019) to compute the $H_2O - CO_2$ continuum. The authors rightly or wrongly assumed that the continuum in the 100-1500 cm^{-1} region, is entirely due to the far wings of the monomer lines. They consequently adjusted a $\chi_{CO_2-H_2O}$ correction factor on the experimental data as was done many years ago for the self- and air-broadened H_2O continua (Clough et al, 1989). In the absence of any other theoretical approach for comparison with our measurements, we used this model, with results displayed in Fig. 2. As can be seen, the agreement between calculations and experiments in the newly studied regions is quite good, which demonstrates the predictive capabilities of the χ factor approach. However, note that concluding from this that the continuum in whole studied regions is only due to the monomer far wings would be highly hazardous.

Finally, the top panel in Fig. 2 enables to compare the H_2O-CO_2 continuum with those, taken from Mlawer et al. (2012), for pure H_2O and H_2O–air. As can be seen the values for H_2O-CO_2 are slightly larger than those for H_2O–air and significantly smaller than those for H_2O-H_2O (Brown et al., 2007). This is consistent with the quasi static predictions of Ma and Tipping (1992) and with the fact that the broadening coefficients of H_2O lines by CO_2 (Brown et al., 2007) are slightly larger than those by air and significantly smaller than those for pure H_2O (Gordon et al., 2022).

5. Conclusion

We measured the H_2O-CO_2 continuum on both sides of the ν_2 absorption band, as well as around 3.1 µm. The data obtained in the spectral range 1100 – 1400 cm^{-1} are consistent with previous measurements (Baranov, 2016; Tran et al., 2019) when their respective uncertainties are taken into account. For the first time, the continuum has been measured on the high frequency side of the ν_2 band from 1800 cm^{-1} to 2000 cm^{-1} as well as between 3100 and 3300 cm^{-1}. In addition to providing new measured data, this study also enabled a successful further test of the $\chi_{H_2O-CO_2}$ factor model proposed in

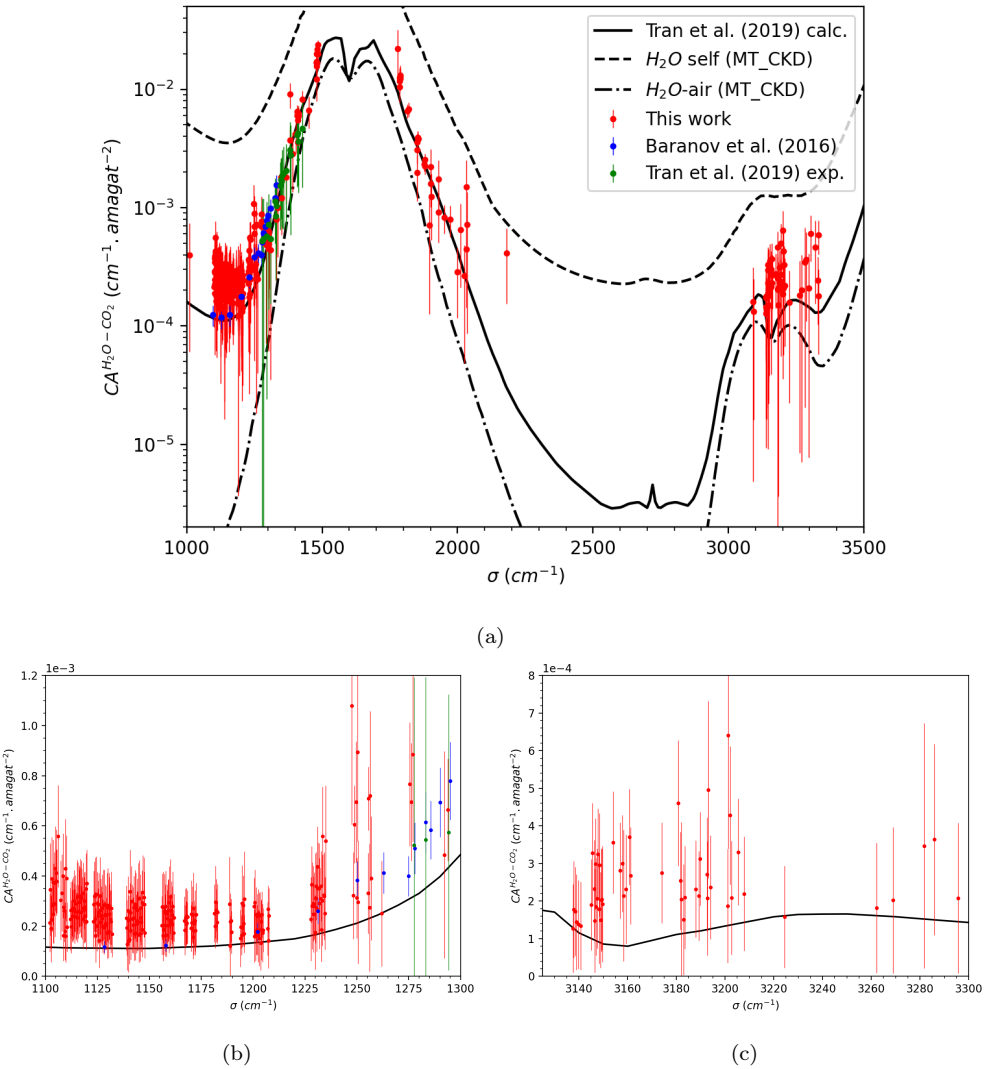

(a)

(b)

(c)

Figure 2: H_2O-CO_2 continuum – The data measured in this study are shown with red dots and are compared to the results of previous experiments (Baranov, 2016; Tran et al., 2019) respectively displayed in blue and green. The black line represents the values predicted using the $\chi_{H_2O-CO_2}$ factor model developed by Tran et al. (2019). For comparison, we also show the self- and air-broadened H_2O far line wings continuum [computed using the latest version available at http://rtweb.aer.com/continuum_frame.html of the MT_CKD model (Mlawer et al., 2012)] with dashed and dashdoted lines, respectively. The top panel (a) displays the results in log scale while the two bottom plots (b) and (c) show respectively the 1100–1300 cm^{-1} and 3100–3300 cm^{-1} regions in linear scale.

Tran et al. (2019). This demonstration of the predictive capabilities of a line-shape correction-factor fitted to experimental results below 1500 cm^{-1} is of considerable interest, particularly for spectral regions where measurements have not yet been made. However recall that our experimental data have been collected at room temperature only, which stresses the crucial need of investigations at various temperatures.

It is worth mentioning that our knowledge of the continua associated with $H_2O - CO_2$ pairs has significantly increased in the last four years, and that much progress has been made after the first computations of Ma et al. (1992) and measurements of Baranov (2016). Many new experimental data have been provided which confirmed the latter data and considerably extended the spectral range in which values of the continuum are available. In addition, the original $\chi_{H_2O-CO_2}$ factor of Ma et al. (1992) has been significantly improved (Tran et al., 2019). This provides a computational approach with which a satisfactory agreement with measurements is obtained at almost all experimentally investigated wavelengths, provided that it is complemented, around 6000 cm^{-1}, by a description (Fleurbaey et al., 2022b) of the collision-induced simultaneous transitions. However, much still remains to be done: First, new measurements are needed to test the model in so far unstudied regions, e.g. 2200 – 3000 cm^{-1}, while experiments of improved precision are desirable around 3.1 µm. Last but not least, the temperature dependence, for which the only information available comes from the early theoretical study of Pollack et al. (1993) must be investigated experimentally.

Declaration of Competing Interest

The authors declare no conflicts of interest

Acknowledgments

This work was performed in the frame of the *Agence Nationale de la Recherche* (ANR) project COMPLEAT (ANR-19-CE31-0010-001). The authors thank Martin Turbet for his contribution by providing the H_2O-CO_2 absorption coefficient using the $\chi_{H_2O-CO_2}$ factor model.

Supplementary material

The measured data of the$H_2O - CO_2$ continuum presented in this work are available in the supplementary material

References

Baranov, Y., Vigasin, A., 1999. Collision-Induced Absorption by CO_2 in the Region of ν_1, $2\nu_2$. J. Mol. Spectroc. 193 (2), 319-325. https://doi.org/10.1006/jmsp.1998.7743.

Baranov, Y., 2016. On the significant enhancement of the continuum-collision induced absorption in H_2O + CO_2 mixtures. J. Quant. Spectrosc. Radiat. Transf. 175, 100-106. https://doi.org/10.1016/j.jqsrt.2016.02.017.

Brown, L.R., Humphrey, C.M., Gamache R.R., 2007. CO_2-broadened water in the pure rotation and ν_2 fundamental regions. J. Mol. Spectroc. 246 (1), 1-21. https://doi.org/10.1016/j.jms.2007.07.010.

Burch, D.E., 1982. Continuum absorption by H_2O. Report AFGL-TR-81-0300, Air Force Geophysics Laboratory, Hanscom AFB, MA.

Burch, D.E., Alt, R.L., 1984. Continuum absorption by H_2O in the 700-1200 cm^{-1} and 2400-2800 cm^{-1} windows. Report AFGL-TR-84-0128, Air Force Geophysics Laboratory, Hanscom AFB, MA.

Clough, S.A., Kneizys, F.X., Davies, R.W., 1989. Line shape and the water vapor continuum. Atmospheric Research, 23, 229-241. https://doi.org/10.1016/0169-8095(89)90020-3.

Fakhardji, W., Tran, H., Pirali, O., Hartmann, J.-M., 2022. Room temperature measurements of the collision-induced absorption by $H_2 + CO_2$ mixtures near 2.4 µm. J. Quant. Spectrosc. Radiat. Transf. 283, 108161. https://doi.org/10.1016/j.jqsrt.2022.108161.

Fleurbaey, H., Campargue, A., Carreira Mendès Da Silva, Y., Grilli, R., Kassi, S., Mondelain, D., 2022a. Characterization of the H_2O + CO_2

continuum within the infrared transparency windows. J. Quant. Spectrosc. Radiat. Transf. 282, 108119. https://doi.org/10.1016/j.jqsrt.2022.108119.

Fleurbaey, H., Mondelain, D., Fakhardji, W., Hartmann, J.-M., Campargue, A. 2022b. Simultaneous collision-induced transitions in H_2O + CO_2 gas mixtures. J. Quant. Spectrosc. Radiat. Transf. 285, 108162. https://doi.org/10.1016/j.jqsrt.2022.108162.

Frommhold, L., 1993. Collision-induced absorption in gases. Cambridge Univ. Press, Cambridge, U. K.

Gordon, I.E., Rothman, L.S., Hargreaves, R.J., Hashemi, R., Karlovets, E.V., Skinner, F.M., Conway, E.K., Hill, C., Kochanov, R.V., Tan, Y., Wcisło,, P., Finenko, A.A., Nelson, K., Bernath, P.F., Birk, M., Boudon, V., Campargue, A., Chance, K.V., Coustenis, A., Drouin, B.J., Flaud, J.–M., Gamache, R.R., Hodges, J.T., Jacquemart, D. , Mlawer, E.J., Nikitin, A.V., Perevalov, V.I., Rotger, M., Tennyson, J., Toon, G.C., Tran, H. , Tyuterev, V.G., Adkins, E.M., Baker, A., Barbe, A., Canè, E., Császár, A.G., Dudaryonok, A., Egorov,O., Fleisher, A.J., Fleurbaey, H., Foltynowicz, A., Furtenbacher,T., Harrison, J.J., Hartmann, J.–M. , Horneman, V.–M., Huang, X., Karman, T., Karns, J., Kassi, S., Kleiner, I., Kofman, V., Kwabia–Tchana, F., Lavrentieva, N.N., Lee, T.J., Long, D.A., Lukashevskaya, A.A., Lyulin, O.M., Makhnev, V.Yu., Matt, W. , Massie, S.T., Melosso, M., Mikhailenko, S.N., Mondelain, D., Müller, H.S.P., Naumenko, O.V., Perrin, A., Polyansky, O.L., Raddaoui, E., Raston, P.L., Reed, Z.D., Rey, M., Richard, C., Tóbiás, R., Sadiek, I., Schwenke, D.W., Starikova, E.,Sung, K., Tamassia, F., Tashkun, S.A., Vander Auwera, J., Vasilenko, I.A., Vigasin, A.A., Villanueva, G.L., Vispoel, B. , Wagner, G., Yachmenev, A. , Yurchenko, S.N. 2022. The HITRAN2020 molecular spectroscopic database. J. Quant. Spectrosc. Radiat. Transf. 277, 107949. https://doi.org/10.1016/j.jqsrt.2021.107949.

Hartmann, J.-M., Boulet, C., Tran, D.D., Tran, H., Baranov, Y., 2018a. Effect of humidity on the absorption continua of CO_2 and N_2 near 4 µm: Calculations, comparisons with measurements, and consequences for atmospheric spectra. J. Chem. Phys. 148, 054304. 10.1063/1.5019994.

Hartmann, J.-M., Tran, H., Armante, R., Boulet, C., Campargue, A.,

Forget, F., Gianfrani, L., Gordon, I., Guerlet, S., Gustafsson, M., Hodges, J. T., Kassi, S., Lisak, D., Thibault, F., Toon, G. C., 2018b. Recent advances in collisional effects on spectra of molecular gases and their practical consequences, J. Quant. Spectrosc. Radiat. Transf. 213 , 178-227 https://doi.org/10.1016/j.jqsrt.2018.03.016.

Karman, T., Gordon, I.E., van der Avoird, A., Baranov, Y.I., Boulet, C., Drouin, B.J., Groenenboom, G.C., Gustafsson, M., Hartmann, J.-M., Kurucz, R.L., Rothman, L.S., Sun, K., Sung, K., Thalman, R., Tran, H., Wishnow, E.H., Wordsworth, R., Vigasin, A.A., Volkamer, R., van der Zande, W.J., 2019. Update of the HITRAN collision-induced absorption section. Icarus, 328, 160-175. https://doi.org/10.1016/j.icarus.2019.02.034.

Lebonnois, S., Eymet, V., Lee, C., Vatant d'Ollone, J., 2015. Analysis of the radiative budget of the Venusian atmosphere based on infrared Net Exchange Rate formalism. J. Geophys. Res. Planets, 120, 1186–1200. doi:10.1002/2015JE004794.

Ma, Q. and Tipping, R.H., 1992. A far wing line shape theory and its application to the foreign-broadened water continuum absorption. III. J. Chem. Phys. 97, 818-828. https://doi.org/10.1063/1.463184.

Mlawer, E.J., Payne, V.H., Moncet, J.-L., Delamere, J.S., Alvarado, M.J., Tobin D.C., 2012. Development and recent evaluation of the MT CKD model of continuum absorption. Phil. Trans. R. Soc. A, 370, 2520–2556. http://doi.org/10.1098/rsta.2011.0295.

Perrin, M.Y. and Hartmann, J.M., 1989. Temperature-dependent measurements and modeling of absorption by $CO_2 - N_2$ mixtures in the far line-wings of the 4.3 µm CO_2 band. J. Quant. Spectrosc. Radiat. Transf. 42 (4), 311-317. https://doi.org/10.1016/0022-4073(89)90077-0.

Pluriel, W., Marcq, E., Turbet, M., 2019. Modeling the albedo of Earth-like magma ocean planets with $H_2O - CO_2$ atmospheres. Icarus, 317, 583-590. https://doi.org/10.1016/j.icarus.2018.08.023.

Pollack, J.B., Dalton, J.B., Grinspoon, D., Wattson, R.B., Freedman, R., Crisp, D., Allen, D.A., Bezard, B., DeBergh, C., Giver,

L.P., Ma, Q., Tipping, R., 1993. Near-Infrared Light from Venus' Nightside: A Spectroscopic Analysis. Icarus, 103, 1-42. https://doi.org/10.1006/icar.1993.1055.

Ptashnik, I. V., Klimeshina, T. E., Solodov, A. A., Vigasin, A. A., 2019. Spectral composition of the water vapour self-continuum absorption within 2.7 and 6.25 µm bands, J. Quant. Spectrosc. Radiat. Transf. 228 , 97-105 https://doi.org/10.1016/j.jqsrt.2019.02.024.

Sung, K., Brown, L.R., Toth, R.A., Crawford, T.J., 2009. Fourier transform infrared spectroscopy measurements of H_2O-broadened half-widths of CO_2 at 4.3 µm. Can. J. Phys. 87 (5), 469-484. https://doi.org/10.1139/P08-130.

Tran, H., Boulet, C. , Stefani, S. , Snels, M., Piccioni, G., 2011. Measurements and modelling of high pressure pure CO_2 spectra from 750 to 8500 cm^{-1}. I— central and wing regions of the allowed vibrational bands. J. Quant. Spectrosc. Radiat. Transf. 112 (6), 925-936 https://doi.org/10.1016/j.jqsrt.2010.11.021.

Tran, H., Turbet, M., Chelin, P., Landsheere, X., 2018. Measurements and modeling of absorption by CO_2 + H_2O mixtures in the spectral region beyond the CO_2 ν_3-band head. Icarus, 306, 116-121. https://doi.org/10.1016/j.icarus.2018.02.009.

Tran, H., Turbet, M., Hanoufa, S., Landsheere, X., Chelin, P., Ma, Q., Hartmann, J.-M., 2019. The CO_2–broadened H_2O continuum in the 100–1500 cm^{-1} region: Measurements, predictions and empirical model. J. Quant. Spectrosc. Radiat. Transf. 230, 75-80. https://doi.org/10.1016/j.jqsrt.2019.03.016.

Turbet, M., Gillmann, C., Forget, F., Baudin, B., Palumbo, A., Head, J., Karatekin, O., 2020. The environmental effects of very large bolide impacts on early Mars explored with a hierarchy of numerical models. Icarus, 335, 113419. https://doi.org/10.1016/j.icarus.2019.113419.

Turbet, M., Bolmont, E., Chaverot, G., Ehrenreich, D., Leconte, J., Marcq, E., 2021. Day–night cloud asymmetry prevents early oceans on Venus but not on Earth. Nature, 598, 276–280.

https://doi.org/10.1038/s41586-021-03873-w.